ELSEVIER

Journal of Organometallic Chemistry 553 (1998) 173–178

Journal of Organometallic Chemistry

para-Fluoro benzyl substituted bis(indenyl) metallocenes as catalyst precursors in ethene polymerization

Gerhard Jany [*], Marina Gustafsson, Timo Repo [1], Erkki Aitola, José A. Dobado, Martti Klinga [2], Markku Leskelä

Laboratory of Inorganic Chemistry, University of Helsinki, P.O. Box 55, FIN-00014 Helsinki, Finland

Received 26 May 1997

Abstract

The unbridged complexes bis(η^5-(1-*para*-fluoro benzyl)indenyl) MCl_2 (**2**: M = Hf; **3**: M = Zr) as well as their ethylene bridged analogues bis[(η^5-3-(1-*para*-fluoro benzyl)indenyl)ethane] MCl_2 (**4**: M = Hf; **5**: M = Zr) have been synthesized and the obtained *rac*- and *meso*-isomers were separated from the 1:1 isomer mixtures. Complexation was performed by converting the ligand precursors (1-*para*-fluoro benzyl)indene (**1a**) and bis(3-(1-*para*-fluoro benzyl)indenyl)ethane (**1b**) into their lithio salts and further treatment with MCl_4. To study the influence of the *para*-fluoro benzyl substituent in ethene polymerization, the catalyst precursors **2–5** were activated with methylalumoxane (MAO) and their polymerization behavior was compared to corresponding unsubstituted metallocenes. The crystal structure of *meso*-like **3** was determined by means of X-ray structure analysis, showing a central/lateral:*gauche*-type orientation of its *para*-fluoro benzyl substituents in the solid state. © 1998 Elsevier Science S.A.

Keywords: Zirconium; Hafnium; Indenyl; Polymerization; Catalysis

1. Introduction

Transition metal Group 4 *ansa*-metallocene dichlorides as catalyst precursors in homogeneous olefin polymerization have extensively been studied, since they opened up a path to obtain polymers with defined microcrystalline structure by the use of a suitable ligand environment around the catalytic active metal center [1–3]. Metallocene (IV) complexes are usually activated by a cocatalyst such as MAO, forming a cationic species which is known to be active in olefin polymerization.

Among other things, the polymerization behavior of metallocenes is strongly depending on the nature and position of the substituents in their ligand framework [1–4]. In this context, we chose the Ind_2MCl_2 and $EtInd_2MCl_2$ metallocene key structures to be altered in 1-position with a sterical demanding and electron withdrawing group. In order to investigate the electronic properties of the substituted indenyl fragment, theoretical calculations were carried out for a variety of potential substituents such as 2,4,6-trichloro benzyl or *para*-fluoro benzyl. [3] We elected the latter one to modify the mentioned bis(indenyl) systems and use them as catalyst precursors in ethene polymerization.

2. Results and discussion

2.1. Syntheses and calculations

A convenient route to obtain indene derivatives bearing a benzyl substituent in 1-position can be performed by reacting indenyl lithium with benzyl halides in polar solvents. For that purpose, we treated the lithio salts of either indene or bis(3-indenyl)ethane with *para*-fluoro benzyl bromide in diethyl ether, which gave the ligand precursors **1a,b** in moderate yields.

[*] Corresponding author.
[1] Also corresponding author.
[2] X-ray diffraction studies.

[3] A more detailed discussion of the performed theoretical studies on 1-substituted indenyl ligand systems will be the subject of a future publication.

Theoretical calculations were performed to evaluate the electronic properties of the isolated (1-*para*-fluoro benzyl)indenyl anion (**1a***) and its parent compound, the unsubstituted indenyl anion. Electrostatic potentials provide information about electron-rich and electron-poor sites inside a molecule, and electrostatic interactions between molecules [5–9]. The numerical values for the electrostatic potentials (calculated for the centre of each five- and six-membered ring) of the indenyl anion are −106 and −127 kcal/mol, whereas the corresponding values for **1a*** are significantly more positive, −66 and −92 kcal/mol, respectively. Piccolrovazzi et al. were able to show that in modified bis(indenyl)-systems such as $(4,7\text{-}F_2\text{Ind})_2ZrR_2$ the electron withdrawing groups lowered both, catalytic activity and molecular weight of the obtained polyethenes, if compared to unsubstituted Ind_2ZrCl_2 [10]. Hence a decrease of the electron density in **1a*** compared to its parent compound should be in accord with a decrease of the electron density of the respective metal complex and thus, affect its polymerization behavior when utilized as catalyst in ethene polymerization. To prove this suggestion, the ligand precursors **1a,b** were converted into their lithio salts and reacted with $HfCl_4$ and $ZrCl_4$ in dichloro methane to form the unbridged metallocene complexes **2** and **3**, as well as the ethylene bridged *ansa*-metallocene complexes **4** and **5**, as displayed in Fig. 1.

All complexes were formed as 1:1 mixtures of their *rac*- and *meso*-isomers and could be separated by fractional crystallization from hot toluene. In the case of **2** and **3,** it was possible to classify the *rac*- and *meso*-like isomers by correlating the solid state structure of *meso*-like **3** (vide post) with the ^{1}H NMR spectra of the complex fractions. The ethylene bridged complexes **4** and **5** could also be separated from their *rac*- and *meso*-mixtures but suitable crystals for X-ray structure analysis were not obtained. The low yields in preparation of **4** and **5** also prevented further functionalization, e.g., into their dimethyl analogues, to identify the fractions of the different structural isomers by means of ^{1}H NMR [11]. For this reason, we only used the unseparated 1:1 isomer mixtures of complexes **2–5** as catalyst precursors for the polymerization of ethene. [4]

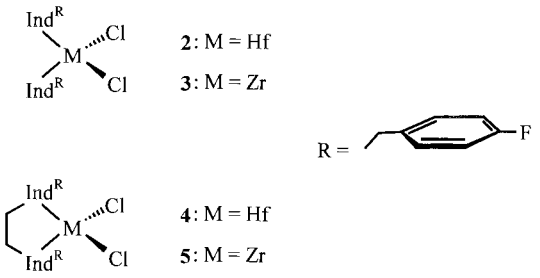

Fig. 1. *para*-Fluoro benzyl substituted bis(indenyl) complexes **2–5** used as catalyst precursors for the polymerization of ethene.

2.2. Polymerization experiments

The metallocene dichlorides **2–5** (Fig. 1), all carrying the sterically demanding and electron withdrawing *para*-fluoro benzyl group as substituent in 1-position of their indenyl moieties, were studied in ethene polymerization at 50°C and 2.0 bar ethene overpressure in toluene after activation with MAO. The resulting polymerization data are summarized in Table 1. Furthermore, a series of literature known complexes (Table 1, entries **6–9**) was synthesized, to compare the polymerization behavior of these parental compounds to the *para*-fluoro benzyl substituted indenyl complexes under similar conditions.

The unbridged hafnium complex **6** produced when activated with MAO high molecular weight polyethene (M_W = 959 kg/mol) with moderate activity, whereas its zirconium analogue **7** exhibited high activity (A = 62500 kg (PE) ([Zr] h)$^{-1}$), but lower M_W instead (Table 1). These observations are in general accordance to studies reported earlier [12–18]. The remarkable difference in activity and M_W, which is exposed by **6** and **7**, diminishes if the *para*-fluoro benzyl group is introduced to the ligand framework. The metallocene complexes **2** and **3** produce only polyethene with reduced activity and M_W about 383 and 366 kg/mol, respectively. Further linking of the substituted indenyl fragments by an ethylene bridge in 3-position affords the *ansa*-metallocene complexes **4** and **5**, which polymerize ethene with even less activity and lower M_W. The decline in activity of complex **4** is rather dramatic and its activity is even below the one found for $EtFlu_2HfCl_2$ (**10**), [5] bearing also two demanding β-substituents on each Cp-fragment. However, the hafnocene **4** now generates polyethene with even lower M_W than the zirconocene **5**. An unusual feature, which was also reported by Alt et al. for the bis(fluorenyl) complex **10** [19,20]. The general decrease in activity and M_W which is caused by catalyst systems **2–5** compared to **6–9**, is corresponding to polymerization results recently published for a similar kind of substituted indenyl systems. While $(1\text{-PhInd})_2ZrCl_2$ still polymerized ethene with

[4] Besides, in the case of ethene, it is less necessary to maintain a certain symmetry (e.g., *rac* or *meso*) throughout the polymerization process, because no stereoregular polymers can be achieved (in contrary to propylene). Exemplary, ethene was polymerized with *rac*-like **2** under similar conditions, showing minor differences in activity and M_W to the 1:1 mixtures (see Table 1). Data of *rac*-like **2**: t_P = 1201 s, [Hf] = 5 μmol, yield = 3.59 g, activity = 2152 kg (PE) ([Hf] h)$^{-1}$, T_m = 124.6°C, M_W = 340 kg/mol, M_W/M_N = 3.1.

[5] Polymerization data of **10** under same conditions (vide supra): t_P = 4134 s, [Hf] = 10 μmol, yield = 3.28 g, activity = 286 kg (PE) ([Hf] h)$^{-1}$, T_m = 124.0°C, M_W = 305 kg/mol, M_W/M_N = 4.3.

Table 1
Ethene polymerization data for catalyst systems bearing *para*-fluoro benzyl substituents (**2–5**/MAO) compared to non-substituted systems (**6–9**/MAO) under similar polymerization conditions[a]

Compound		t_P^b (s)	[M[c]] (μmol)	Yield (g)	Activity[d]	T_m^e (°C)	M_W (kg/mol)	M_W/M_N
(*p*-Fluoro)Ind_2HfCl_2	(**2**)	1007	5	3.70	2645	122.3	383	2.9
(*p*-Fluoro)Ind_2ZrCl_2	(**3**)	1026	2	3.89	6824	119.4	366	3.4
Et[(*p*-Fluoro)Ind_2]$HfCl_2$	(**4**)	3621	10	1.54	153	125.7	109	2.5
Et[(*p*-Fluoro)Ind_2]$ZrCl_2$	(**5**)	1852	10	7.57	1473	125.4	115	4.4
Ind_2HfCl_2	(**6**)	924	5	10.0	7812	124.2	959	2.6
Ind_2ZrfCl_2	(**7**)	1014	0.5	8.8	62 500	124.3	490	2.3
rac-$EtInd_2HfCl_2$	(**8**)	1354	5	3.95	2101	120.6	387	4.4
rac-$EtInd_2ZrCl_2$	(**9**)	1822	2	9.49	9377	121.7	240	3.2

[a] Ethene overpressure 2.0 bar, polymerization temperature 50°C and MAO excess of [Al]: [M] = 5000:1.
[b] Polymerization time.
[c] M = Zr, Hf.
[d] kg (PE) ([M] h)$^{-1}$.
[e] Onset melting temperatures of the polymers after pre-heating the samples up to 200°C and cooling down again to 70°C (cooling rate 10°C/min).

moderate activity, the introduction of a second phenyl group in 3-position reduced the catalytic activity of the complex about 20 times [21].

We attribute that the major reason for the observed loss in activity and lower M_W obtained with compounds **2–5** can be found in a sterical interference between the *para*-fluoro benzyl substituents, the monomer and the polymer chain. Fig. 2 illustrates how the *para*-fluoro benzyl group might restrict the coordination sphere around the catalytic active metal center, even in the unlinked metallocenes. It is most likely that a potential electron withdrawing effect of the *para*-fluoro benzyl substituent only plays a minor role in polymerization.

Our current work is focused on using the isolated, stereorigid *rac*- and *meso*-like diastereoisomers of the unbridged metallocenes **2** and **3** for the stereospecific polymerization of propylene [11,22,23].

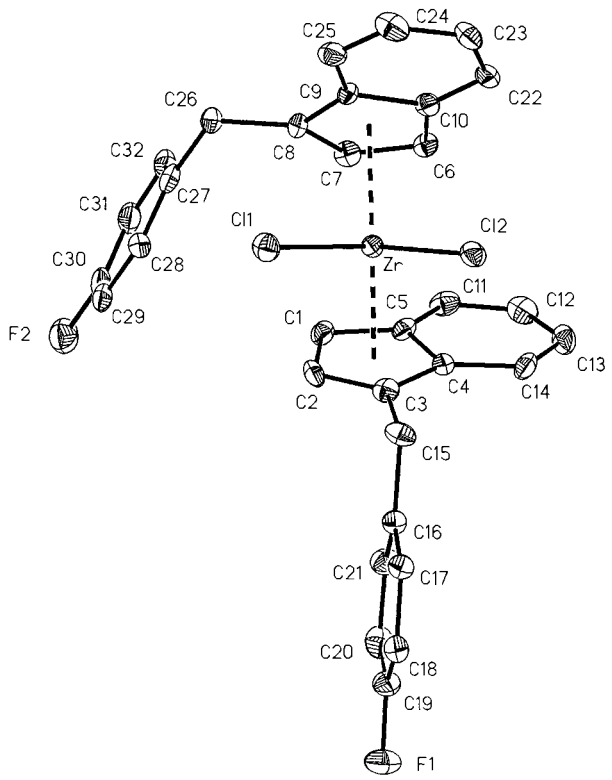

Fig. 2. Solid state structure of *meso*-like complex **3**. Hydrogen atoms are omitted for clarity.

3. Solid state structure

Table 2 summarizes the bonding parameters of *meso*-like **3**: Its Zr–Cl as well as the Zr–Cp distances around the pseudotetrahedrally coordinated metal centre correspond to the ones reported for Ind_2ZrCl_2 (**7**) and *meso*-like $[Cy(IndH^4)]_2ZrCl_2$ (**11**) [24] in the solid state. Also the Cp1–Zr–Cp2 angle ($\phi = 129.0°$) correlates with the values found for **7** (128.3°) and **11** (130.5°). The distances between zirconium and the Cp-carbon atoms of **3** range from 2.449(9) Å to 2.650(9) Å which indicates no deviation from normal η^5:η^5 coordination (Fig. 2) [25].

The alterations from perpendicularity to the Zr–Cp

Table 2
Selected bonding parameters for *meso*-like **3**

Zr–C11	2.417(3) Å	Zr–C12	2.429(3) Å
Zr–Cp1	2.218(11) Å	Zr–Cp2	2.242(11) Å
C3–C15	1.50(2) Å	C15–C16	1.524(13) Å
C8–C26	1.492(12) Å	C26–C27	1.53(2) Å
C11–Zr–C12	94.6(1)^0	ϕ, Cp1–Zr–Cp2[a]	129.0^0
C15–Cp1–Cp2–C26[b]	100.6^0	C4–Cp1–Cp2–C9[b]	103.6^0
β, Cp1–Zr[c]	2.3^0	β, Cp2–Zr[c]	5.7^0
θ[d]	55.5^0		

[a] Bending angle.
[b] Dihedral angle.
[c] Deviation from perpendicularity to the Zr–Cp vector.
[d] Angle between the two Cp-planes.

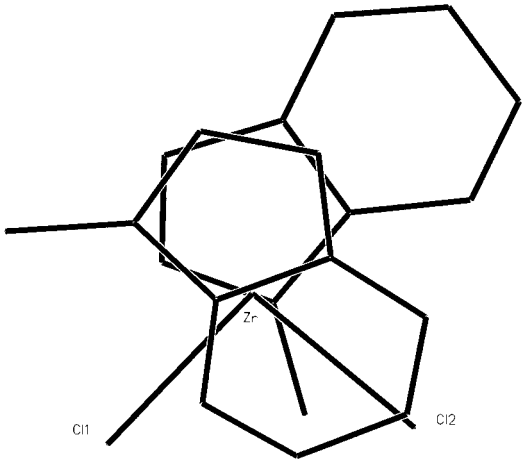

Fig. 3. Ligand framework of *meso*-like complex **3** in the solid state, projected onto the Cl–Zr–Cl plane. Hydrogen atoms and the two *para*-fluoro benzyl units are omitted for clarity.

vectors, β, are comparable to the ones found for **7**, whereas the angle between the two Cp-planes, θ, is reduced from 59.3(2)° to 55.5(4)° when indenyl is substituted in 1-position by a *para*-fluoro benzyl fragment. [6] In the solid state of *meso*-like **3**, the *para*-fluoro benzyl substituents point towards the same direction, showing a C15–Cp1–Cp2–C26 dihedral angle of 100.6°. To further correlate the structure of *meso*-like **3** to the one of *meso*-like **11**, another dihedral angle (C4–Cp1–Cp2–C9 = 103.6°) was chosen, displaying only a minor deviation from the one reported for *meso*-like **11** (105.1°) by Krüger et al. and the same central/lateral: *gauche* type orientation is exhibited in Fig. 3 [24,26,27].

4. Experimental

4.1. Materials

All preparative reactions were carried out under an atmosphere of dry argon by using standard Schlenk techniques. Et_2O, toluene and alkanes were purified by distillation from sodium. CH_2Cl_2 was distilled from CaH_2. Methylalumoxane (MAO, 30 wt.% solution in toluene) was purchased from Borealis Polymers Oy. Compounds **6** [28], **7** [28], **8** [12], **9** [29–31] and **10** [19] were prepared according to modified literature procedures. ^{1}H and ^{13}C NMR spectra were recorded on a Varian Gemini 2000, chemical shifts are referenced with respect to TMS. [7] Mass spectra (EI, HRMS) were acquired by JEOL JMS-SX102. Elemental analysis were determined via Heraeus VT-CHN-Rapid. DSC measurements were performed on a Perkin Elmer DSC-2, calibrated with indium, tin and lead (temperature scanning rate 20°C/min). Molecular weights (M_W) and molecular weight distributions (M_W/M_N) of the polyethene samples were determined by GPC (Waters 150C ALC/GPC) in 1,2,4-trichloro benzene relative to polystyrene standards.

4.2. Polymerizations

In a 1-l Büchi glass autoclave 300 ml of toluene and cocatalyst (MAO) were added, thermostated (50°C), charged up with ethene overpressure (2.0 bar) and mixed with the desired amount of complex solution. The monomer pressure ($\pm$50 mbar) and temperature ($\pm$0.5°C) were kept constant during each polymerization run. Monomer consumption, inside temperature and pressure were controlled by real time monitoring. The polymerizations were stopped and the polyethenes precipitated quantitatively by pouring the solution into 600 ml of methanol, acidified with aqueous hydrochloric acid. The samples were washed several times with methanol and dried at 70°C.

4.3. Syntheses

4.3.1. Synthesis of the ligand precursors ***1a,b***

To a solution of either 5.8 ml indene (50 mmol) or 6.45 g bis indenyl ethane (25 mmol) in 200 ml Et_2O, *n*-butyllithium (31.25 ml, 1.6 M in hexane) was added dropwise at 0°C. The reaction mixture was stirred for 2 h in an ice bath and the reaction completed by the addition of 6.23 ml (50 mmol) *para*-fluoro benzyl bromide. After further stirring overnight at ambient temperature, an aqueous solution of NH_4Cl (200 ml) was added and the organic layer thoroughly extracted with Et_2O. The ether was distilled off and the crude product chromatographed on silica gel [eluent: pentane (**1a**), hexane (**1b**)] giving **1a,b** as colorless sticky oils.

1a (5.15 g, 22.9 mmol, 45.9%): MS(EI) m/z: 224 (M^+). HRMS(EI) Calcd for $C_{16}H_{13}F$: 224.101. Found: 224.0999. ^{1}H NMR (200 MHz, $CDCl_3$): δ = 2.76 (dd, 1H, J = 8.8/4.6/9.0 Hz, CH_2), 3.12 (dd, 1H, J = 6.6/7.0/6.8 Hz, CH_2), 3.68–3.76 (m, 1H, CHInd), 6.47 (d, 1H, J = 4.0 Hz, CHInd), 6.85 (d, 1H, J = 3.8 Hz, CHInd), 6.9–7.4 (m, 8 H, aromatic H). Anal. Calcd for $C_{16}H_{13}F$: C, 85.68; H, 5.84. Found: C, 85.48; H, 5.77.

[6] The reported θ value of **7** in Ref. [36] is given for the whole indenyl moieties. If only the angle between the two Cp-planes is considered, it diminishes from 62.07(15)° to 59.3(2)°.

[7] Exemplary, the ^{13}C NMR shifts for *rac*- and *meso*-like **2** are given: ^{13}C NMR (200 MHz, $CDCl_3$) *rac*-like **2**: δ = 31.97, 95.05, 113.96, 114.38, 118.08, 120.70, 122.72, 123.81, 124.50, 124.62, 124.98, 125.53, 128.97, 129.13, 134.47, 134.53, and *meso*-like **2**: δ = 32.08, 94.81, 114.04, 117.89, 119.37, 122.67, 123.35, 124.48, 124.58, 126.41, 129.10, 129.34, 134.11, 134.18.

1b (4.91 g, 10.3 mmol, 41.4%): MS(EI) *m/z*: 474 (M^+). HRMS(EI) Calcd for $C_{34}H_{28}F_2$: 474.2147. Found: 474.2171. ^{1}H NMR (200 MHz, $CDCl_3$): δ = 2.56–2.73 (m, 2H, CH_2), 2.84 (s, 4H, CH_2), 2.97–3.14 (m, 2H, CH_2), 3.53–3.71 (m, 2H, CH), 6.12 (s, 2H, CH), 6.6–7.4 (m, 16 H, aromatic H). Anal. Calcd for $C_{34}H_{28}F_2$: C, 86.05; H, 5.94. Found: C, 86.21; H, 5.80.

*4.3.2. Synthesis of the catalyst precursors **2–5***

2.25 g (10 mmol) of the ligand precursor **1a** or 2.37 g (5 mmol) of **1b** were converted into their corresponding lithio salts by treatment with 6.25 ml *n*-butyllithium (1.6 M in hexane) at 0°C. After stirring for 30 min at ambient temperature the ether was distilled off and the solid residue cooled down to −78°C. A total of 200 ml of pre-cooled (−78°C) CH_2Cl_2 were added followed by an addition of 5 mmol MCl_4 (**2** and **4**: M = Hf; **3** and **5**: M = Zr). The suspension was stirred overnight and allowed to come to room temperature. The reaction mixture was filtered through Celite and the solvent evaporized. The solid residue was washed with hexane and further extracted with hot toluene (100 ml). Crystallization from toluene at −20°C yielded to colorless **2** and **4** and lemon–yellow colored **3** and **5**.

2 (3.47 g, 4.37 mmol, 87.4%): MS(EI) *m/z*: 692–698 (with appropriate isotope ratio for $C_{32}H_{24}F_2HfCl_2^+$), 473 (M^+ − **1a**). ^{1}H NMR (200 MHz, $CDCl_3$): δ *rac* = 4.14 (q, 4H, J = 16.2/28.2/16.0 Hz, CH_2), 5.73 (d, 2H, J = 3.0 Hz, CHInd), 5.94 (d, 2H, J = 3.4 Hz, CHInd), 6.8–7.7 (m, 16 H, aromatic H), and δ *meso* = 4.26 (d, 4H, J = 9.0 Hz, CH_2), 5.19 (d, 2H, J = 3.2 Hz, CHInd), 6.26 (d, 2H, J = 3.2 Hz, CHInd), 6.8–7.7 (m, 16 H, aromatic H). Anal. Calcd for $C_{32}H_{24}F_2HfCl_2$: C, 55.23; H, 3.47. Found: C, 55.43; H, 3.60.

3 (2.42 g, 3.98 mmol, 79.6%): MS(EI) *m/z*: 605–613 (with appropriate isotope ratio for $C_{32}H_{24}F_2ZrCl_2^+$), 387 (M^+ − **1a**). ^{1}H NMR (200 MHz, $CDCl_3$): δ *rac* = 4.13 (q, 4H, J = 16.0/23.8/16.0 Hz, CH_2), 5.87 (d, 2H, J = 3.0 Hz, CHInd), 5.99 (d, 2H, J = 2.6 Hz, CHInd), 6.8–7.75 (m, 16 H, aromatic H), and δ *meso* = 4.22 (d, 4H, J = 3.0 Hz, CH_2), 5.35 (d, 2H, J = 3.2 Hz, CHInd), 6.28 (d, 2H, J = 3.4 Hz, CHInd), 6.8–7.7 (m, 16 H, aromatic H). Anal. Calcd for $C_{32}H_{24}F_2ZrCl_2$: C, 63.14; H, 3.97. Found: C, 63.66; H, 3.89.

4 (0.89 g, 1.24 mmol, 24.8%): MS(EI) *m/z*: 720–726 (with appropriate isotope ratio for $C_{34}H_{26}F_2HfCl_2^+$). ^{1}H NMR (200 MHz, $CDCl_3$): δ = 3.99–4.10 (m, 4H, CH_2), 4.26 (d, 4H, J = 3.8 Hz, CH_2), 6.05 (s, 2H, CHInd), 6.8–7.7 (m, 16 H, aromatic H), and δ = 3.57–3.68 (m, 4H, CH_2), 3.77 (d, 4H, J = 3.8 Hz, CH_2), 5.90 (s, 2H, CHInd), 6.8–7.7 (m, 16 H, aromatic H. Anal. Calcd for $C_{34}H_{26}F_2HfCl_2$: C, 56.56; H, 3.62. Found: C, 57.24; H, 3.99.

5 (0.57 g, 0.89 mmol, 17.9%): MS(EI) *m/z*: 631–639 (with appropriate isotope ratio for $C_{34}H_{26}F_2ZrCl_2^+$). HRMS(EI) Calcd for $C_{34}H_{26}F_2ZrCl_2$: 632.0410. Found: 632.0457. ^{1}H NMR (200 MHz, $CDCl_3$): δ = 3.90–4.03 (m, 4H, CH_2), 4.19 (s, 4H, CH_2), 6.03 (s, 2H, CHInd), 6.7–7.6 (m, 16 H, aromatic H), and δ = 3.48–3.59 (m, 4H, CH_2), 3.70 (d, 4H, J = 3.8 Hz, CH_2), 5.95 (s, 2H, CHInd), 6.7–7.6 (m, 16 H, aromatic H). Anal. Calcd for $C_{34}H_{26}F_2ZrCl_2$: C, 64.34; H, 4.12. Found: C, 66.11; H, 4.12.

4.4. X-ray crystallographic studies

The crystal data of *meso*-like **3** were collected on a Rigaku AFC-7S single crystal diffractometer at 193(2) K using Mo–Kα radiation (graphite monochromatized, scan type w/2Θ). Intensities were corrected for Lorentz and polarization effects and for absorption (0.89 < 1.00). Solution: Direct methods combined with subsequent Fourier analysis. All non-hydrogen atoms were refined anisotropically. Hydrogen atoms were refined isotropically on calculated positions (riding model). Suitable crystals for X-ray determination were obtained by recrystallization from hot toluene. Crystal dimensions 0.45 × 0.35 × 0.20 mm; a = 10.332(5), b = 11.687(5), c = 21.600(6) Å, $\alpha = \beta = \gamma = 90°$, V = 2608(2) Å^3, crystal system orthorhombic, space group $P2_12_12_1$ (No. 19), Z = 4, mol mass 608.63 g/mol, D(calcd) = 1.550 g/cm^3, λ = 0.71073 Å, data collection range θ = 2.57 to 26.49°, reflections collected 2800, independent reflections 2800, reflections refined 2778, goodness-of-fit on F^2 = 1.050, $R1$ = 0.0605 and $wR2$ = 0.1424 (2298 with $I_o > 2\sigma I_o$), $R1$ = 0.0776 and $wR2$ = 0.1575 (all data). The largest difference peak and hole in the final residual electron density map situates in the vicinity of zirconium (0.838 and −1.422 e Å^{-3}). Calculations were carried out with the SHELXTL/PC and SHELXL-93 program systems [32,33].

4.5. Computational methods

Semi-empirical calculations were performed using the PM3 Hamiltonian [34,35] included in SPARTAN 4.0 program [37], running on a Silicon Graphics O2 workstation. All the stationary points were fully optimized (without imposition of any geometrical restriction for compound **1a*** and C_{2v}-symmetry for the indenyl anion). After optimization of the structures, vibrational analyses were carried out to check the nature of the stationary points (no imaginary frequencies were found indicating that the structures were true minima). Default options were applied in the calculation of the electrostatic potentials.

5. Supporting information available

Structure determination summaries, complete tables of atomic coordinates, bond lengths and angles,

anisotropic displacement coefficients and hydrogen atom for *meso*-like **3** (9 pages). Ordering information is given on any current masthead page.

Acknowledgements

We are obliged to Arja Lehtinen (GPC), Markku R. Sundberg (for assistance in performing theoretical calculations) and Ulf Dietrich (elementary analysis). General support from Borealis Polymers Oy is gratefully acknowledged. This work has been partially funded by the Academy of Finland, Technology Development Centre (TEKES) and the Center for International Mobility (CIMO). G.J. extends his thanks to N. Ogre, C. Key and D.R. Goettel.

References

[1] M. Farina, TRIP 2 (1994) 80.
[2] H.H. Brintzinger, D. Fischer, R. Mülhaupt, B. Rieger, R. Waymouth, Angew. Chem. 107 (1995) 1255.
[3] M. Bochmann, J. Chem. Soc., Dalton Trans. (1996) 255.
[4] P.C. Möhring, N.J. Coville, J. Organomet. Chem. 479 (1994) 1, and literature cited there.
[5] W.J. Hehre, Practical Strategies for Electronic Structure Calculations, Wave function, Irvine, CA, USA, 1995, pp. 195–214.
[6] L.E. Chirlian, M.M. Francl, J. Comput. Chem. 8 (1987) 894.
[7] C.M. Breneman, K.B. Wiberg, J. Comput. Chem. 11 (1990) 361.
[8] S.D. Kahn, C.F. Pau, W.J. Hehre, J. Am. Chem. Soc. 108 (1986) 7381.
[9] S.D. Kahn, W.J. Hehre, J. Am. Chem. Soc. 109 (1987) 663.
[10] N. Piccolrovazzi, P. Pino, G. Consiglio, A. Sironi, M. Moret, Organometallics 9 (1990) 3098.
[11] T.K. Han, S.C. Yoon, Y.S. Ko, B.W. Woo, J.T. Park, S.I. Woo, Polym. Bull. 37 (1996) 35.
[12] J.A. Ewen, L. Haspeslagh, J.L. Atwood, H. Zhang, J. Am. Chem. Soc. 109 (1987) 6544.
[13] A. Ahlers, W. Kaminsky, Makromol. Chem., Rapid Commun. 9 (1988) 457.
[14] K. Heiland, W. Kamninsky, Makromol. Chem. 193 (1992) 601.
[15] W. Kamninsky, R. Engehausen, K. Zoumis, W. Spaleck, J. Rohrmann, Makromol. Chem. 193 (1992) 1643.
[16] J. Koivumäki, Polym. Bull. 34 (1995) 413.
[17] W. Kaminsky, Macromol. Chem. Phys. 197 (1996) 3907.
[18] A. Fries, T. Mise, A. Matsumoto, H. Ohmori, Y. Wakatsuki, Chem. Commun. (1996) 783.
[19] H.G. Alt, W. Milius, S.J. Palackal, J. Organomet. Chem. 472 (1994) 113.
[20] H.G. Alt, Russ. Chem. Bull. 44 (1995) 1.
[21] P. Foster, J.C.W. Chien, M.D. Rausch, Organometallics 15 (1996) 4951.
[22] G. Erker, R. Nolte, Y.-H. Tsay, C. Krüger, Angew. Chem. 101 (1989) 642.
[23] E. Polo, M.L.H. Green, F. Benetello, G. Prini, S. Sostero, O. Traverso, J. Organomet. Chem. 527 (1997) 173.
[24] C. Krüger, F. Lutz, M. Nolte, G. Erker, M. Aulbach, J. Organomet. Chem. 452 (1993) 79.
[25] C. Kowala, J.A. Wunderlich, Acta Crystallogr. B32 (1976) 820.
[26] G. Erker, M. Aulbach, M. Knickmeier, D. Wingbermühle, C. Krüger, M. Nolte, S. Werner, J. Am. Chem. Soc. 115 (1993) 4590.
[27] M. Knickmeier, G. Erker, T. Fox, J. Am. Chem. Soc. 118 (1996) 9623.
[28] E. Samuel, M.D. Rausch, J. Am. Chem. Soc. 95 (1973) 6263.
[29] F.R.W.P. Wild, L. Zsolnai, G. Huttner, H.H. Brintzinger, J. Organomet. Chem. 232 (1982) 233.
[30] J.A. Ewen, J. Am. Chem. Soc. 106 (1984) 6355.
[31] W. Kaminsky, K. Külper, H.H. Brintzinger, F.R.W.P. Wild, Angew. Chem., Int. Ed. Engl. 24 (1985) 507.
[32] G.M. Sheldrick, SHELXTL/PC. Siemens Analytical X-ray Instruments, Madison, WI, USA, 1990.
[33] G.M. Sheldrick, SHELXL-93, University of Göttingen, 1993.
[34] J. Stewart, J. Comput. Chem. 10 (1989) 209.
[35] J. Stewart, J. Comput. Chem. 10 (1989) 221.
[36] T. Repo, M. Klinga, I. Mutikainen, S. Yincai, M. Leskelä, M. Polamo, Acta Chem. Scand. 50 (1996) 1116.
[37] SPARTAN version 4.0, Wave function, 18401 Von Karman Ave., #370 Irvine, CA 92715 USA.© 1995 Wave function.